

# Multiwavelength blazar variability from radio to TeV photon energies on timescales ranging from decades to minutes

Arti Goyal

in collaboration with - Ł. Stawarz, M. Ostrowski, S. Zola, M. F. Aller, H. D. Aller, T. Hovatta, A. Lahteenmäki, S. Jorstad and A. Marscher, et al.,

Astronomical Observatory of the Jagiellonian University, Poland

18 September 2018

# Stochastic blazar variability

- Random, aperiodic intensity variations across **ALL** wavebands and on **ALL** timescales.

- The typical shape of power spectral density (PSD;  $P(\nu_k) \propto \nu_k^{-\beta}$ ) is a power-law (COLORED NOISE;

$\beta \sim 1 - 3$ )—stochastic process.

- Is the process stationary in time?

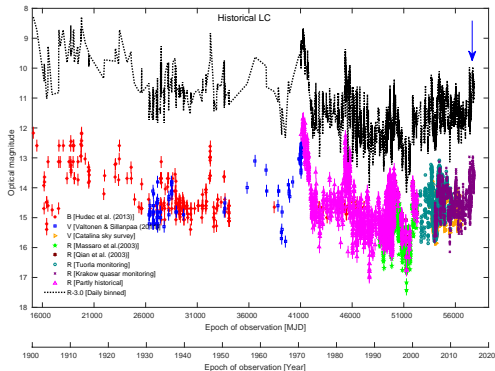
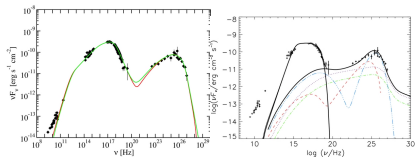
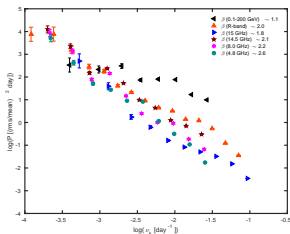


Figure 1: 117 year-long optical light curve (LC) of OJ 287 (Goyal et al., 2018)

# Synchrotron and IC-dominated spectral regions



**Figure 2:** Spectral energy distribution (SED) of Mrk 421 from Abdo et al. (2010a) (*left*: Leptonic scenario) and (*right*: Hadronic scenario)



**Figure 3:** PKS 0735+178 (Goyal et al. 2017)

## Problems with SED fitting:

- 1) Too simplified model setup (single-zone SSC model) – NO **‘characteristic/relaxation’** timescale.
- 2) Lack of statistically significant correlations (Max-Moerbeck et al. 2014, Lindfors et al. 2016; **Exceptions** Hovatta et al. 2014, Fuhmann et al. 2016)
  - *Fermi*-LAT energies:  $\beta \sim 1$  (Flicker/pink-noise)!
  - Radio/optical energies:  $\beta \sim 2$  (Brownian/red-noise)!

# Variability spectrum from years to minutes timescale

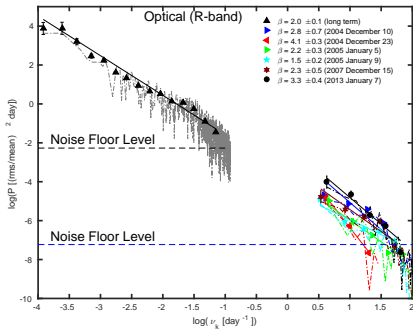


Figure 4: PKS 0735+178 (optical energies; Goyal et al. 2017).

- Optical energies:  $\beta \sim 2$  (long-term) and  $\beta \sim 1-3$  on minutes timescale!
- $\gamma$ -ray energies:  $\beta \sim 1$  (long-term) and  $\beta \sim 1$  on minutes timescale!
- NO change in normalization!

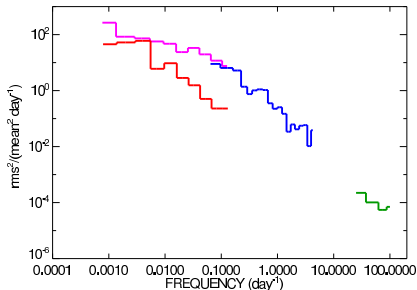


Figure 5: 3C 279 (*Fermi*-LAT energies; Ackermann et al. 2016).

# Minute-like flare of PKS 2155–304

Yet,

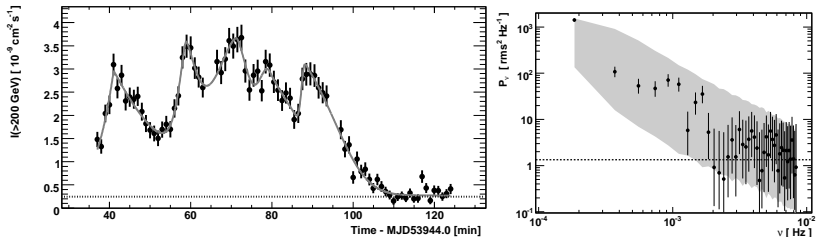


Figure 6: PKS 2155-304 (Aharonian et al., 2007).

- H.E.S.S. energies  $\beta \sim 2$  (red noise!) on intra-night timescales vs.  $\beta \sim 1$  on years to weeks timescales (Abdalla et al. 2017).
- $\Rightarrow$  Nature of variability process changes on  $\sim$  daily timescales.

# Data acquisition and analysis methods

- **TeV- $\gamma$ -rays**: H.E.S.S. and VERITAS ( $\geq 200$  GeV)
- **GeV- $\gamma$ -rays**: *Fermi*-LAT (0.1-300 GeV) satellite
- **X-rays**: *Swift*-XRT (0.3-10 keV) and *RXTE*-PCA (3-20 keV) satellites
- **Optical frequencies** : SMARTS, Tuorla and Kepler satellite
- **Radio frequencies** : UMRAO (4.8, 8, 14.5 GHz), OVRO (15 GHz) and MRO (22 and 37 GHz)

## **Determination of statistical properties of light curves using PSDs:**

- LC analysis in Fourier-domain: Discrete Fourier Transform (DFT; Uttley et al., 2002, Max-Moerbeck et al. 2014, Goyal et al. 2017) – **Biases due to red-noise leak, aliasing and uneven sampling.**
- LC analysis in time-domain: modeling the LC as a continuous-time auto regressive moving average process (CARMA; Kelly et al. 2014, Goyal et al. 2018) – implies that variability is a stationary stochastic process (NOT necessarily true for blazar sources). **NEXT STEP – ARIMA modeling (Zhang et al. 2018).**

# CARMA modeling of OJ 287

## Continuous-time Auto Regressive

**Moving Average:**  $y(t)$  is the solution to the stochastic differential equation

$$\frac{d^p y(t)}{dt^p} + \alpha_{p-1} \frac{d^{p-1} y(t)}{dt^{p-1}} + \dots + \alpha_0 y(t) = \beta_q \frac{d^q \epsilon(t)}{dt^q} + \beta_{q-1} \frac{d^{q-1} \epsilon(t)}{dt^{q-1}} + \dots + \epsilon(t), \quad (1)$$

where  $\epsilon(t)$  is the Gaussian “input” white noise with zero mean and variance  $\sigma^2$ ,  $\alpha$ 's and  $\beta$ 's are AR and MA coefficients. The corresponding power spectrum

$$P(f) = \sigma^2 \left| \sum_{j=0}^q \beta_j (2\pi i f)^j \right|^2 \left| \sum_{k=0}^p \alpha_k (2\pi i f)^k \right|^{-2} \quad (2)$$

$\Rightarrow \gamma$ -rays are relaxed on timescale of  $\sim 150$  days.

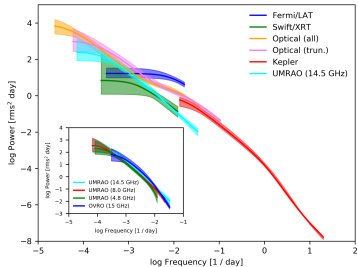


Figure 7: PSD of OJ 287 (Goyal et al.

2018)

# Different methods for PSD generation

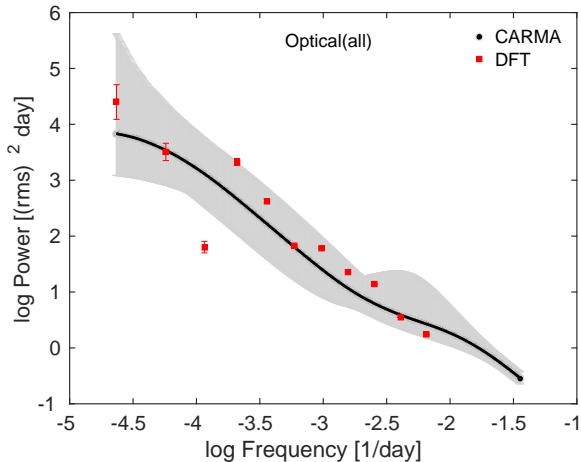


Figure 8: PSD of OJ 287 (Goyal et al. 2018)

=> Comparable results from Fourier and time-domain analysis!



# Multiwavelength LCs including TeV

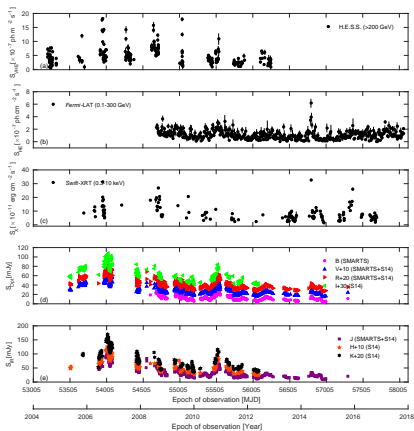


Figure 9: PKS 2155–304 (TeV from HESS; thanks to David Sanches)

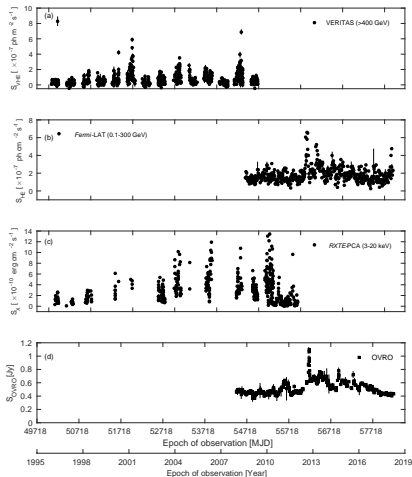


Figure 10: Mrk 421 (TeV from Acciari et al., 2014)

# Squared fractional variance

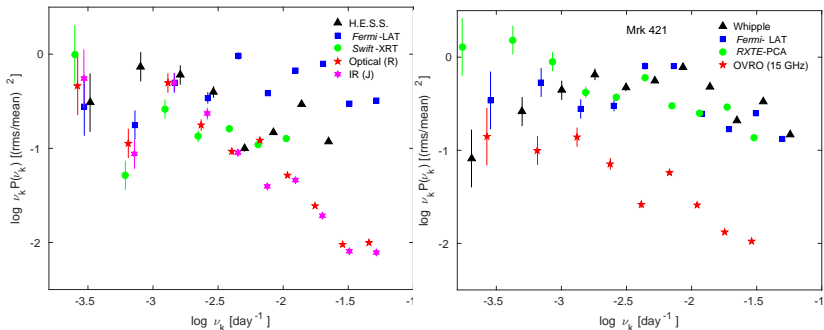


Figure 11: Squared fractional as a function of timescale. PKS 2155–304 (left) and Mrk 421 (right).

- In this representation:  $\beta \sim 0$  for keV/GeV/TeV frequencies (pink noise) and  $\beta \sim 1$  for radio/optical frequencies (red-noise)!
- Fractional variance does not increase with frequency for these HBLs on timescales ranging from years for weeks!
- Against the expectations of single one-zone model!

# Fourier-resolved spectroscopy (FRS) or rms spectra

- rms as a function of radiation frequency for difference timescales corresponds to FRS spectra (First applied in the context of X-ray binaries; Revnivtsev et al. 1999).

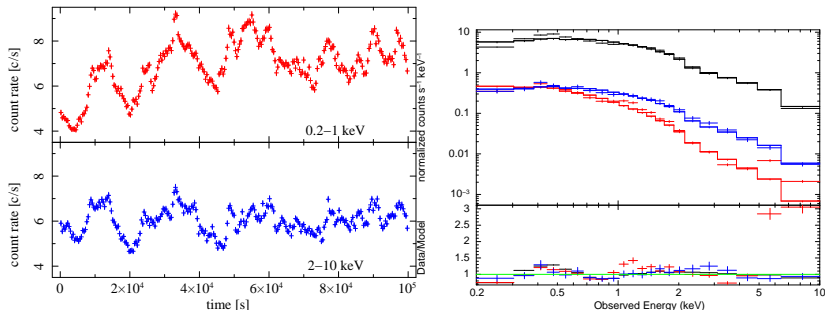


Figure 12: Seyfert galaxy NGC 3227 (Arevalo & Markowitz 2014). *left*: LC. *right*: rms spectra for soft frequencies (red) and hard (blue) and total (black).

=> Two spectral components: (1) hard with  $\Gamma \sim 1.7$  dominating on  $<30$ ks timescales and (2) soft with  $\Gamma \sim 3.0$  dominating on  $>30$ ks timescales.

# rms spectra for blazars 3C 279 and PKS 1510–089

=> Good spectral and temporal coverage is mandatory!

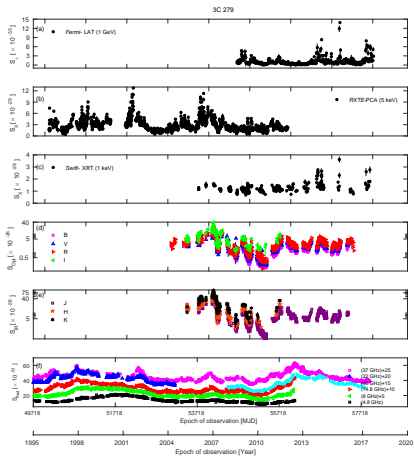


Figure 13: MWL LCs of 3C 279

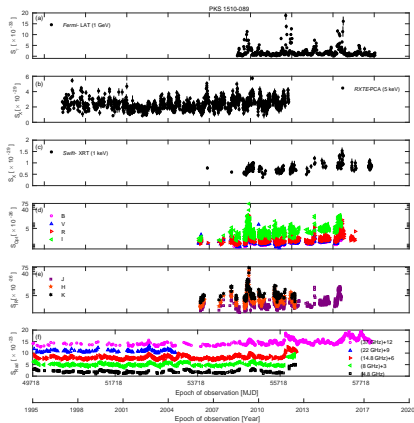


Figure 14: MWL LCs of PKS 1510–089

# rms spectra on years/months/weeks timescales

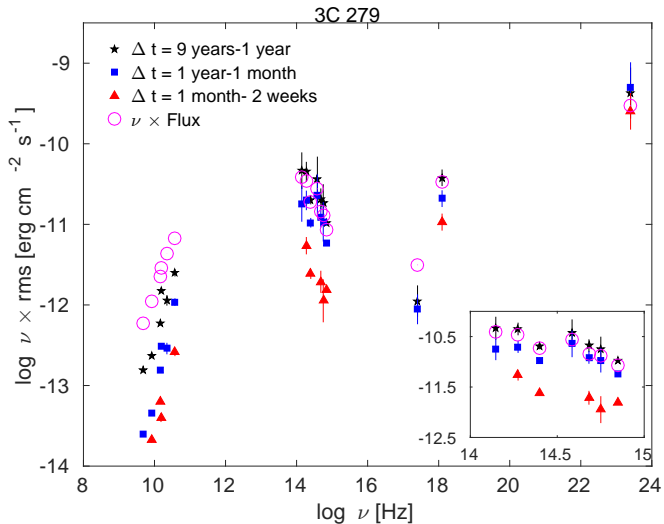


Figure 15: rms spectra of 3C 279

# rms spectra on years/months/weeks timescales

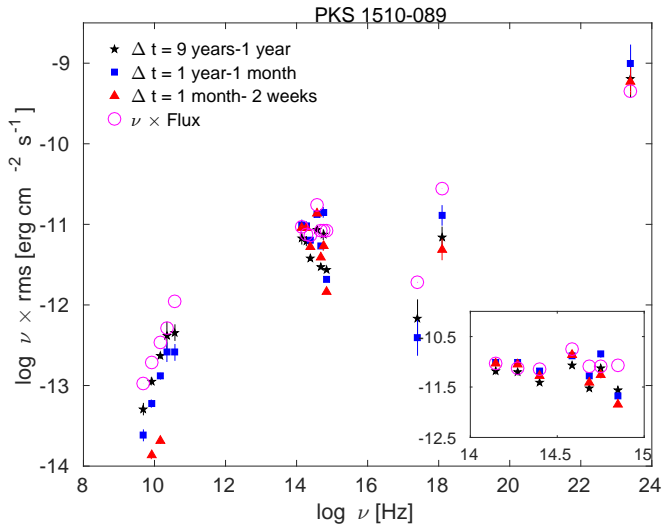


Figure 16: rms spectra of PKS 1510–089

# Results

## PSD analysis

- Featureless, single power-law power spectral density over timescales ranging from 5-6 decades in temporal frequency range.
  - Detection of relaxation timescale of  $\sim 150$  days for the  $\gamma$ -rays (OJ 287), not seen at lower energies—inhomogeneous jet!
  - Hints of non-stationarity on hourly timescales!
- Statistical character of  $\gamma$ -ray and X-ray variability (flicker/pink) is different than that of optical and radio (damped/red).
- Results supported for different blazars;  $\gamma$ -ray (Sobolewska et al., 2014), X-rays by Isobe et al. (2015), optical (Kastendieck et al. 2011), Max-Moerbeck et al. (2014).
- BL Lac objects – single zone SSC modeling(?)

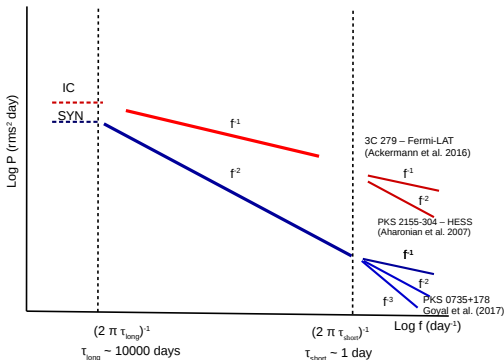
# Results

## rms spectra

- The largest variance at each frequency is on the longest timescale, along to the expectations of strictly colored-noise PSDs from years to weeks timescales.
  - rms is gradually increasing from weeks to months to years timescales for the blazar, however, the exact dependence appears to be different for different photon energies.
  - Fractional variability is  $\sim 100\%$  on years/months/weeks timescales at *Fermi*-LAT energies.
- 
- NO QPOs!
  - Different spectral components—varying in both normalization and slope— emission from extended volumes of jet with different particle populations, magnetic fields, bulk Lorentz factors, external radiation density.



# Different relaxation timescales and non-stationarity !



Synchrotron variability is driven by a single stochastic process with the relaxation timescales  $\tau_{\text{long}} \gtrsim 1,000$  days ( $\rightarrow$  red noise for the variability timescales shorter than  $\tau_{\text{long}}$ ), while  $\gamma$ -ray variability is driven by a superposition of stochastic processes with relaxation timescales  $\tau_{\text{long}} \gtrsim 100$  days and  $\tau_{\text{short}} \lesssim 1$  day ( $\rightarrow$  pink noise for the variability timescales between  $\tau_{\text{long}}$  and  $\tau_{\text{short}}$ , and red noise for the variability timescales shorter than  $\tau_{\text{short}}$ ).